

# Size distribution of CdS nanocrystal-doped silica xerogels

A. OTHMANI, J. C. PLENET, E. BERNSTEIN, F. PAILLE, C. BOVIER,  
J. DUMAS

*Département de Physique des Matériaux, UA 172 CNRS, Université Claude Bernard,  
43, Boulevard du 11 Novembre 1918, 69622 Villeurbanne, Cedex, France*

C. MAI

*Groupe d'Etude de Métallurgie Physique et de Physique des Matériaux, UA 341, CNRS,  
Institut National des Sciences Appliquées, 43, Boulevard du 11 Novembre 1918,  
69622 Villeurbanne, Cedex, France*

Pure and porous silica xerogels doped with CdS nanocrystals have been prepared by a sol–gel process. In order to determine parameters convenient for non-linear optical properties, particle size distributions were obtained by two complementary techniques: transmission electron microscopy (conventional, CTEM, and high resolution, HRTEM) and small angle X-ray scattering (SAXS). Monolithic samples having CdO concentrations varying from 5 to 20 wt % have been studied. Details are given of an image analysis technique used to study the CTEM micrographs.

## 1. Introduction

Ultrasmall semiconductor particles have gained considerable attention in recent years because of their enhanced non-linear optical properties and photocatalytic properties [1, 2]. The observation of photo-induced blue shifts in the absorption spectra and excitation peak [3] is evidence of quantum size effects due to the confinement of electronic excitations inside nanocrystals. Since Jain and Lind reported high non-linear optical properties of  $\text{CdS}_x\text{Se}_{(1-x)}$  doped glass [4], much work has been carried out on this type of material [5]. One of the main problems encountered in the characterization of samples doped with nanocrystals is the measurement of the mean particle diameter value and determination of the particle size distribution. This information is essential in order to improve the quality of samples for use in non-linear optical experiments or devices [6].

In the present work, a sol–gel route for the preparation of silica gel doped with high concentrations of CdS nanocrystals is reported, and two characterization methods allowing the monitoring of nanocrystal sizes are discussed. The nanocrystal structure is determined by high resolution transmission electron microscopy (HRTEM). The size distribution of the nanocrystals is determined by small angle X-ray scattering (SAXS) and conventional transmission electron microscopy (CTEM).

## 2. Experimental procedure

### 2.1. Sample preparation

Conventional melting to produce semiconductor-doped glass uses multicomponent oxides in order to

reduce the glass transition temperature. In fact, it does not allow a Cd concentration above about 1 wt % [7], due to the volatility and instability of CdO species which occurs at temperatures around 900 °C.

The sol–gel process is a suitable technique for producing a chemically well defined matrix of pure silica at temperatures lower than 500 °C [8, 9], and for the preparation of specimens containing concentrations of CdO up to 20% by weight. The CdS doped gel samples are obtained by a two-step method [8] which involves the use of three solutions:

1. an acid solution, A, containing tetraethyl-orthosilicate (TEOS), ethanol, water and hydrochloric acid in the molar proportion 1:1:1:0.27;
2. a basic solution, B, consisting of water, ethanol and ammonium hydroxide in molar proportions of 4:1.25:0.005;
3. a doping solution, C, consisting of 0.05 mol hydrated cadmium acetate dissolved in 1 mol methanol. The preparation was carried out in two stages:

1. In the first stage, a pure silica glass was produced by a sol–gel technique, slightly modified in order to incorporate the cadmium compound within the structure. The doping solution C was mixed with solution A, stirred carefully and left for 2 h to hydrolyse. Solution B was then added and carefully mixed. The resulting liquid was left in a closed container for ten days and then the temperature was raised by  $5^\circ\text{C h}^{-1}$  to 500 °C and held at this level for 4 h. Mixing of the different components of the initial solution had to be made in the ratio

$$(1 \text{ volume of solution A} + n \text{ volume of solution C}) \\ + 1 \text{ volume of solution B}$$

A value  $n = 0.1$  for 1 mol of TEOS gave roughly a 1 wt % Cd-doped xerogel, and the amount of Cd was adjusted by the quantity  $n$ . The concentration is given by the ratio (weight of CdO/weight of  $\text{SiO}_2$ ). In this paper results for samples containing 5, 10, 15 and 20 wt % concentrations are presented.

2. The second step of the preparation is thermal treatment in an  $\text{H}_2\text{S}$  atmosphere, at  $200^\circ\text{C}$  for 2 h, in order to precipitate CdS microcrystals in the silica gel matrix. The sample then takes on a characteristic light yellow colour. The glass obtained has an apparent density of 1.75 when no Cd is added. Samples are typically  $15 \times 15$  mm, with thickness ranging from 0.1 to 5 mm depending on experimental conditions.

## 2.2. Electron microscopy

Thin foils for transmission electron microscopy were obtained from the bulk material by first mechanical polishing and then ion thinning. High resolution and conventional observations were carried out in a Jeol 200CX-UHP2S electron microscope, operating at 200 kV, with a point-to-point resolution of 0.22 nm.

The CdS nanocrystals appear in the microscope as a fringe system, which is a representation of the phase contrast originating from coherent scattering of the electron beam by the periodic nanocrystal potential. Fig. 1 is a typical example of a CdS nanocrystal observed. The texture of the background, which comes from the amorphous matrix, can be eliminated by Fourier transformation-based filtering (Fig. 2). The plane distances are obtained from the direct image or from the separation of spots on the diffraction pattern obtained by Fourier transformation: hexagonal structure (wurtzite) of bulk CdS is observed on all nanocrystals visualized. No attempt was made to obtain a crystal size distribution from these high resolution images.

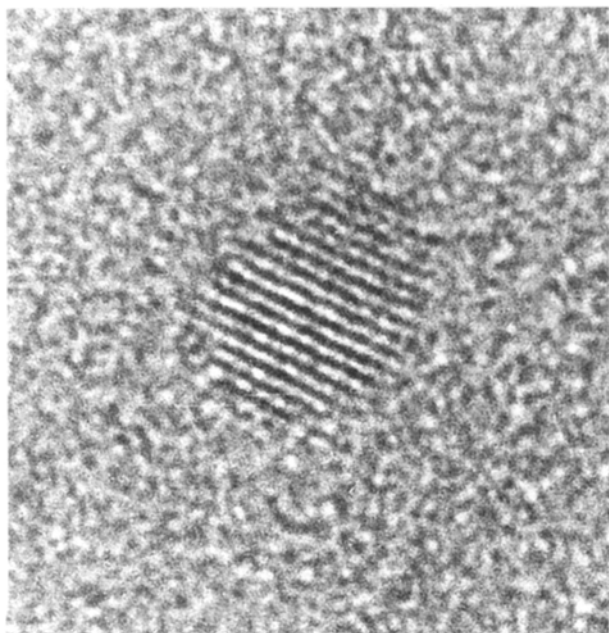


Figure 1 HRTEM view of a typical CdS nanocrystal.

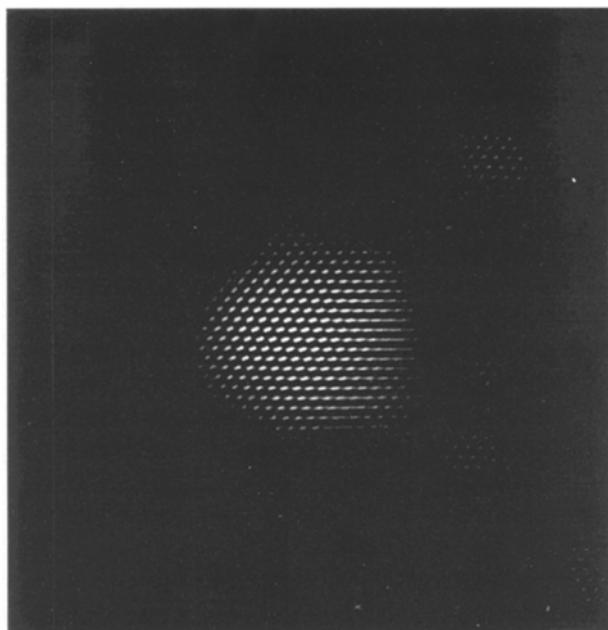


Figure 2 Fourier filtered HRTEM image of a CdS particle.

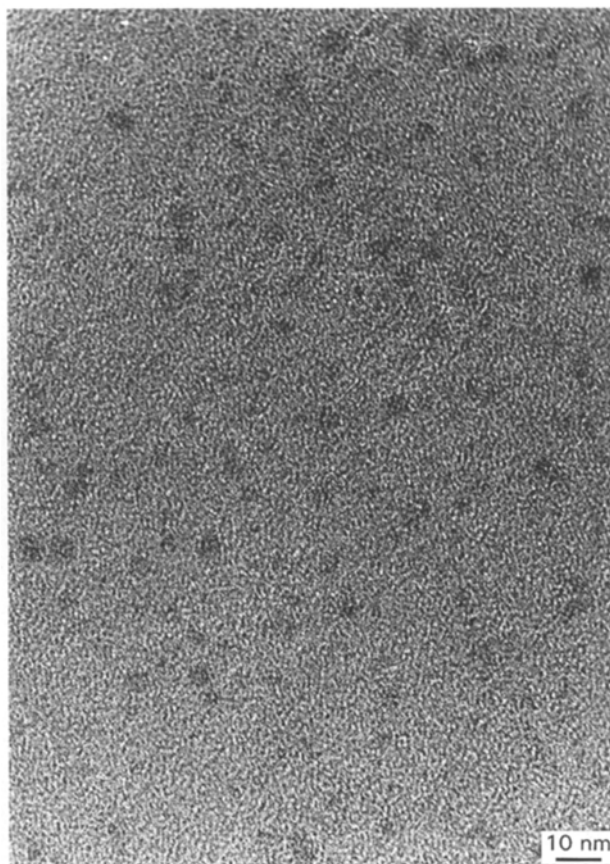


Figure 3 Conventional TEM image of CdS nanocrystals.

Conventional transmission electron microscopy (CTEM) was used to observe a greater area of the sample, to be able to determine a size distribution from an image analysis method. In Fig. 3, which shows a sample at a magnification  $\times 160\,000$ , 375 particles are viewed on the same image and their area individually measured. The contrast is poor and a certain amount of morphological filtering is done by an

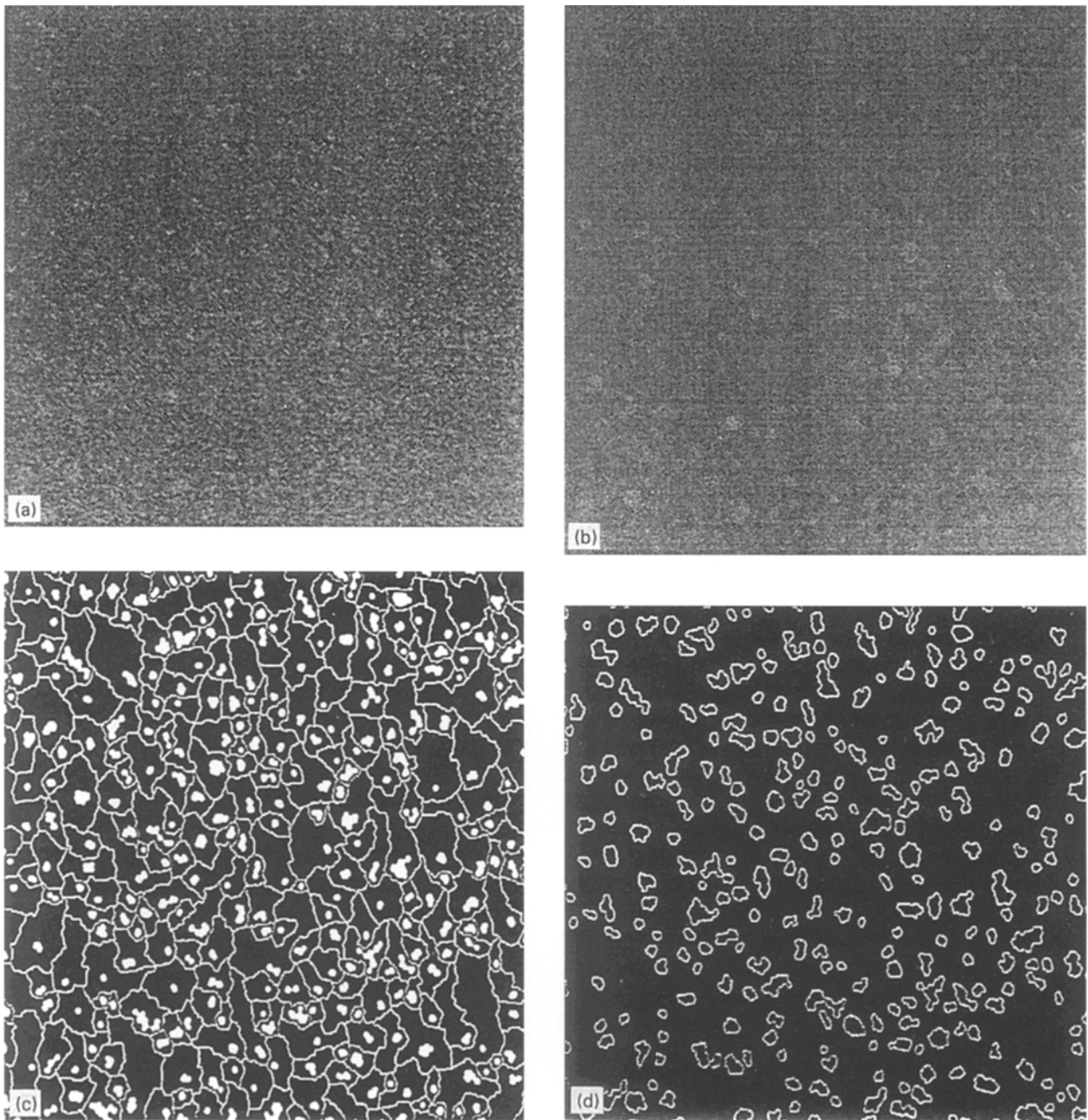


Figure 4 Morphological fitting of CTEM image: (a) initial image used for calculation, (b) result of alternating sequential filters, (c) markers used in gradient watershed, and (d) particle boundaries.

alternate sequential procedure [10, 11] to clean the image before the computation: this non-linear filtering eliminates part of the noise and some particles smaller than 4 pixels wide, i.e. around 1.2 nm in diameter. The different steps of the method are summarized on Fig. 4.

Contour detection is done by taking into account the contrast and the width of edges between the background and the particles, and by calculating the gradient of the image which is higher along these luminance transitions. The particle area is slightly minimized by this method. The diameter of an equivalent circle is calculated for each particle and its histogram, shown on Fig. 5, gives a mean diameter around 4 nm. The very small number of particles observed with larger sizes ( $\sim 8$  nm) is probably due to poor separation of two or more nanocrystals during the image segmentation procedure.

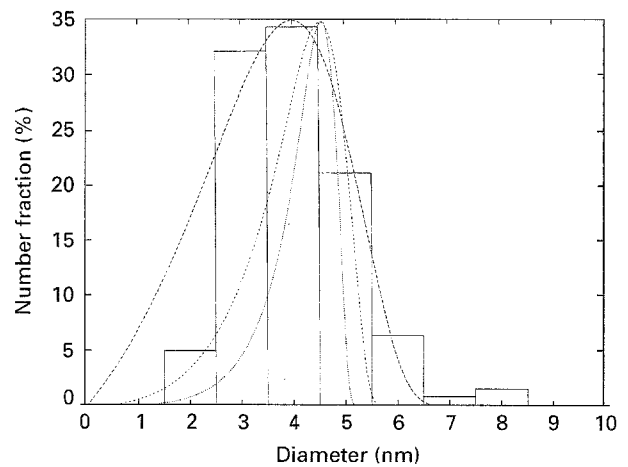


Figure 5 Diameter histogram of 375 CdS particles in 20%, Cd xerogel (—). Distributions calculated from the LSW theory for 3 different diffusion behaviours: (---) surface, (-·-·) bulk, and (····) grain.

### 2.3. Small angle X-ray scattering (SAXS)

SAXS measurements were performed on a Rigaku high power rotating anode generator with a position sensitive detector. A multi channel analyser connected to a microcomputer allows fast measurements. The X-ray wavelength beam 0.154 nm CuK<sub>α1</sub>, is focused on the detector plane by a curved monochromator and is held under vacuum in order to reduce air scattering.

Two experimental conditions have been used for SAXS experiments. First, a series of measurements has been done with a sample-detection distance of 1 m. At this distance, the diffusion spectra (Fig. 6) show a correlation feature for the four concentrations of xerogels treated by H<sub>2</sub>S, which has been analysed by a method described elsewhere [12] to obtain the particle size distribution and the average distance between particles. Fig. 7 shows this distribution for the four concentrations studied: according to these measurements, the same conditions of preparation and treatment with H<sub>2</sub>S give a size distribution which does not depend on CdS concentration. This strengthens the Low Frequency Inelastic Raman Scattering (LOFIRS) results which lead to the same conclusion [13]. The average distance between CdS clusters decreases when the CdO concentration increases (Table I): the number of clusters increases with CdO concentration, without a corresponding increase of their size.

As a Guinier plot cannot be used when spectra show correlation features, a second series of measurements has been done with 0.27 m distance to check the former results by calculation of the Porod radius using the asymptotic behaviour at the high  $q$ -value of the

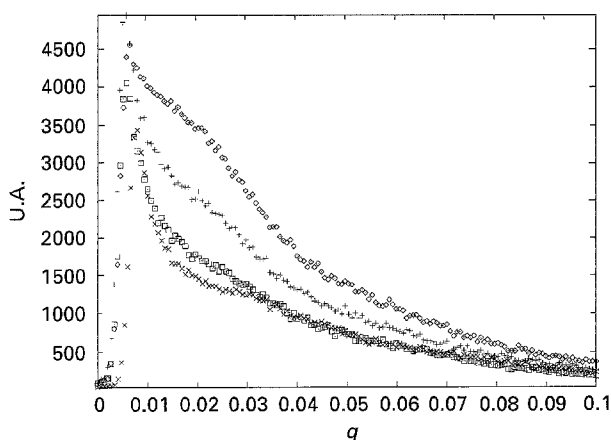


Figure 6 SAXS diffusion spectra of H<sub>2</sub>S-treated samples with (◇) 5%, (+) 10%, (□) 15%, and (×) 20% Cd concentrations.

TABLE I Parameters deduced from SAXS measurements and used for size analysis. Distances between CdS clusters for various Cd concentrations

Concentration	Diameter (nm)	$q_1$ value (cf. text)	Cluster distance (nm)
20% before H <sub>2</sub> S exposure	1.4	0.225	–
5%	3.8	0.225	34.2
10%	4.8	0.225	30.8
15%	4.8	0.234	26.4
20%	4.2	0.213	21.5

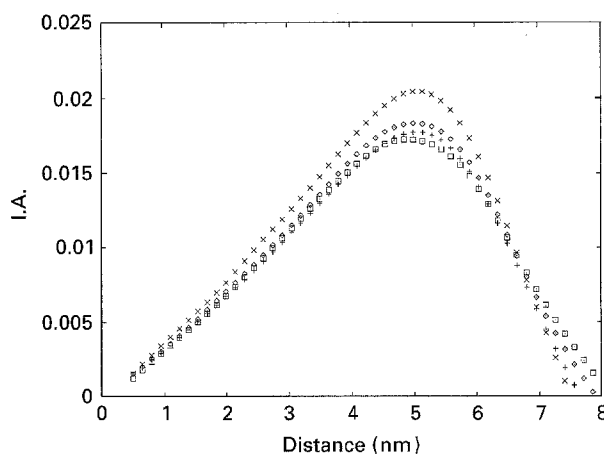


Figure 7 SAXS nanocrystal diameter distribution for H<sub>2</sub>S-treated with (◇) 5%, (+) 10%, (□) 15%, and (×) 20% Cd concentrations.

diffusion curve [14]. This method uses two hypotheses.

1. Integrated diffusion is proportional to the total volume of the scattering particles.
2. At this small distance, the maximum  $q$ -value obtained is in the Porod region. The diffusion, due to the electron density discontinuity at the matrix-particle interface, is related to the surface and is a function of structural details of the interface.

Expecting asymptotically an  $I(q) = A/q^4 + B$  intensity variation for large  $q$ , the  $A$  coefficient is given by the  $[I(q)q^4]$  limit for  $q = 0$  in an  $[I(q)q^4 - q^4]$  plot. This method can be used if the slope  $B$  is close to zero, indicating a smooth interface: it is the case with the 15 and 20% samples. If this condition is not very well fulfilled, as in the 5 and 10% samples, the interface is considered rough and the method cannot be applied with the same confidence. In any case, the  $A$  and  $B$  coefficients are sensitive on the choice of the linear region, between wavenumbers  $q_1$  and  $q_2$ , in the  $I(q)q^4 - q^4$  plot: the particle diameter has been calculated with an  $A$ -value which minimizes  $B$  and the result is shown in Table I. The 1.4 nm diameter is obtained for a 20% sample before any treatment by H<sub>2</sub>S: this value gives an indication of the gel microporosity.

### 3. Discussion

The theoretical size distributions calculated from the Lifschitz, Slezov and Wagner (LSW) theory of Ostwald ripening [15] have been drawn on the particle diameter histogram (Fig. 5). Three cases corres-

ponding to different limiting diffusion processes have been considered. The first one is referred to as the surface reaction case, when evaporation and condensation are the rate-controlling processes. The second and third processes refer to situations in which diffusion is the rate-limiting step, in the bulk and along grain boundaries, respectively. In the approach used [16], the grain boundaries are modelled by cylindrical tubes in which the diffusing species can move: this assertion seems to be convenient for taking into account the mesoporosity of the medium. In the xerogel, nanocrystal growth can be interpreted in terms of two processes: evaporation–condensation on the surface of each nanoparticle and matter transport through the porous texture. On Fig. 5, the best fit is obtained with the first case, especially for the largest sizes. The slight discrepancy on the small size range could be a consequence of the filtering process, which introduces a cut-off around 1.5 nm: the nanocrystal size distribution is governed by the surface reaction step.

#### 4. Conclusions

The sol–gel technique may be used to obtain doped silica xerogels containing high concentrations of CdS nanocrystals. The mean diameter and the size distribution of the particles are important parameters if these samples are to be used in non-linear optical measurements.

Two methods of measuring these parameters are presented to characterize these materials by these size parameters: CTEM gives information on the particle size distribution and HRTEM on the nanocrystal structure. The SAXS technique allows two data treatments which are discussed.

The particle diameter values obtained by the two methods are in a quite good agreement and seem to be

roughly independent of the CdS concentration as has been already shown by the LOFIRS technique [13].

#### Acknowledgements

The authors would like to thank Pr. Jacques Mugnier for fruitful discussions.

#### References

1. Y. WANG, *J. Phys. Chem.* **95** (1991) 1119.
2. E. VOGEL, M. J. WEBER and D. M. KROI, *Phys. Chem. of Glass* **32** (1991) 231.
3. A. I. EKIMOV, and A. A. ONUSHCHENKO, *Sov. Phys. Semicond.* **16** (1982) 757.
4. R. K. JAIN and R. C. LIND, *J. Opt. Soc. Am.* **73** (1983) 647.
5. B. CHAMPAGNON, B. ANDRIANASOLO, A. RAMOS, M. GANDAIS, M. ALLAIS, J. P. BENNOIT, *J. of Appl. Physics* **73** (1993) 2775.
6. H. SHINOJIMA, J. YUMOTO AND N. UESIGI, *Appl. Phys. Lett.* **60** (1992) 298.
7. N. F. BORRELLI, D. W. HALL, H. J. HOLLAND and D. W. SMITH, *J. Appl. Phys.* **61** (1987) 5399.
8. M. NOGAMI, M. WATABE and K. NAGASAKA, *Sol. Gel Optics* **119** (1990) 1328.
9. M. NOGAMI, K. NAGASAKA and E. KATO, *J. Am. Ceram. Soc.* **73** (1990) 2097.
10. S. BEUCHER, *Segmentation d'images et morphologie mathématique*. (ENSMP Fontainebleau (France) Thesis 1990.
11. J. SERRA, (editor), *Image analysis and Mathematical morphology: theoretical advances*. Academic Press, London.
12. C. MAI, F. LIVET, G. VIGIER, *Scripta Metallurgica* **15** (1981) 1179.
13. A. OTHMANI, C. BOVIER, J. C. PLENET, J. DUMAS, B. CHAMPAGNON and C. MAI, *Mater. Science and Eng.* **A168** (1993) 263.
14. V. A. HACKLEY, M. ANDERSON and S. SPOONER, *J. Mater. Res.* **7** (1992) 2555.
15. M. KAHLWEIT, *Adv. Colloid and Interface Sci.* **5** (1975) 1.
16. S. J. JAIN and A. E. HUGHES, *J. of Materials Science* **13** (1978) 1611.

Received 2 August 1993  
and accepted 6 July 1994